Journal of Colloid and Interface Science 512 (2018) 21–28

Contents lists available at ScienceDirect

Journal of Colloid and Interface Science

journal homepage: www.elsevier.com/locate/jcis

Regular Article

Nonenzymatic flexible field-effect transistor based glucose sensor fabricated using NiO quantum dots modified ZnO nanorods

Da-Un-Jin Jung [1], Rafiq Ahmad [1], Yoon-Bong Hahn *

School of Semiconductor and Chemical Engineering, Nanomaterials Processing Research Center, Chonbuk National University, 567 Baekjedaero, Deokjin-gu, Jeonju-si, Jeollabuk-do 54896, Republic of Korea

HIGHLIGHTS

- A non-enzymatic flexible FET based glucose biosensor was fabricated.
- Grown ZnO NRs between source-drain were modified with NiO QDs by sputtering.
- An enhanced electrocatalytic features were recorded for glucose detection.
- The proposed sensor showed wide-linear range, high sensitivity and a low detection limit.
- Successfully used for human whole blood sample and serum sample analysis.

GRAPHICAL ABSTRACT

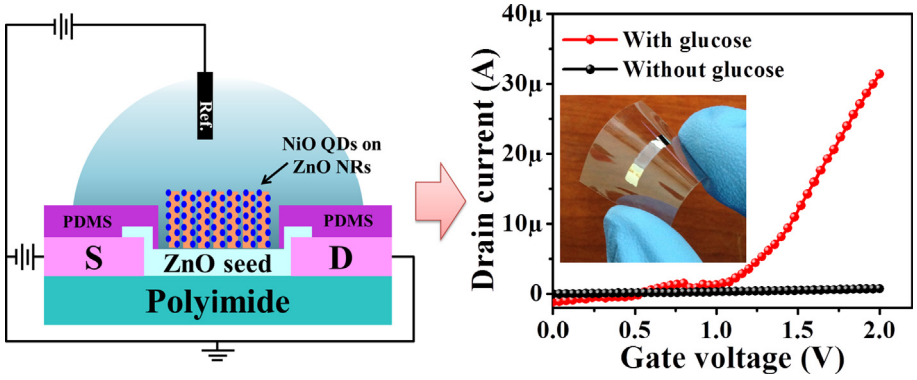

ARTICLE INFO

Article history:
Received 17 August 2017
Revised 11 September 2017
Accepted 10 October 2017
Available online 12 October 2017

Keywords:
Flexible field-effect-transistor
Nonenzymatic glucose biosensor
NiO quantum dots
ZnO nanorods

ABSTRACT

Herein, we fabricated nonenzymatic flexible field-effect transistor (f-FET) based glucose sensor using nickel oxide quantum dots (NiO QDs) modified zinc oxide nanorods (ZnO NRs). The ZnO NRs surfaces were coated with NiO QDs using radio frequency (RF) magnetron sputtering to enhance the electrocatalytic feature and the surface area of ZnO NRs. Under physiological conditions (pH 7.4), the nonenzymatic f-FET glucose sensor shows two linear ranges of 0.001–10 mM and 10–50 mM with the high sensitivity of 13.14 μA cm^{-2} mM^{-1} and 7.31 μA cm^{-2} mM^{-1}, respectively, along with good selectivity, stability and repeatability during glucose detection. The examination of human whole blood and serum samples reveal that the nonenzymatic f-FET based glucose sensor is capable of measuring glucose concentration efficiently in the presence of interfering species and thus can be offered as a promising device for further applications in clinical and non-clinical fields.

1. Introduction

Diabetes is one of the major health concerns with the worldwide prevalence and is predicted to be double to 300 million by 2025 [1]. Diabetic patients suffer from high blood glucose levels due to insulin deficiency that leads to the long-term damage and failure of various organs mainly heart, kidney, eyes, and blood vessels [2,3]. Among several approaches used for glucose

Abbreviations: Nf, Nafion; PET, polyethylene terephthalate; GOx, glucose oxidase; PANI, polyaniline; PAA, poly(acrylic acid); PDAB, poly(1,2-diaminobenzene); PMMA, poly methyl methacrylate; CPNTs, carboxylated polypyrrole nanotubes.

* Corresponding author.
E-mail address: ybhahn@chonbuk.ac.kr (Y.-B. Hahn).

[1] These authors contributed equally to this work.

https://doi.org/10.1016/j.jcis.2017.10.037
0021-9797/

concentration measurement, electrochemical based techniques have got enormous attention due to their high sensitivity, low production cost, simple instrumentation, and rapid response [4–8]. Recently, various attempts have been made for nonenzymatic detection of glucose with rapid response and accurate measurements using different electrochemical based methods [9–15]. The field-effect transistors (FETs) utilizing different nanostructures provide a robust and economically feasible platform in order to achieve high current amplification with sustainable and enhanced signal-to-noise ratio compared to other detection methodologies. Due to their excellent sensitivity and real-time measurement capability for bio- and chemical molecules, FET-based sensors are getting considerable interest.

A variety of metals and metal oxides (e.g. Au, Pd, Ag, Cu, Pt, Ni, CuO, Fe_2O_3, NiO, CoO, $CoWO_4$, MnO_2, TiO_2, etc.,) have been explored for direct glucose oxidation on the electrode surface (without using enzymes) [10–14,16–22]. Metal electrodes, especially Pt and Au are highly electroactive and can easily cause poisoning or fouling of the electrode surface and may result in low sensitivity and poor selectivity in glucose detection. Also, the cost of these metals needs to be considered. Ni-based materials have been extensively studied as electrode materials for nonenzymatic sensors because they can catalyze the electrocatalytic oxidation of glucose [23–29]. However, no work has been reported on nonenzymatic flexible FET based glucose sensor using NiO QDs modified ZnO NRs.

There is certainly room for the improvement in glucose sensing, probably the most frequent clinical measurement made by both clinicians and individuals needing to monitor blood glucose on a regular basis. Moreover, for measurements made outside the clinical laboratory, it is necessary to integrate the sampling and sample handling into the device. There is no interest in adjusting the pH or converting whole blood into serum unless the process is handled automatically. However, most of the nonenzymatic sensors require highly alkaline solutions (pH > 10). Therefore, considerable attentions are needed to develop the nonenzymatic electrodes that exhibit high electrocatalytic activity toward glucose oxidation under physiological conditions. This will help to make implantable sensing devices. Recently, Gao et al. fabricated electrochemical nonenzymatic glucose sensor using PtNi alloy NP-graphene composite that works under physiological conditions (pH 7.4) [29].

For the nonenzymatic sensors, sensitivity, selectivity, and stability are the three main issues that have to be solved. However, these analytical performances could be enhanced largely with the nanostructure material modification. A noble metal-semiconductor modification is the most popular system because of its wide application in sensors, where the metal in contact with the semiconductor greatly enhance the sensor performance [30–32]. Among the large group of semiconductors, ZnO has been used extensively for the development of sensors/biosensors due to their high specific surface area [33,34]. Recently, vertically-oriented ZnO nanostructures on electrode surfaces are getting more attention because they offer the larger surface area for modification and enzyme immobilization and thus enhance the sensing performance of fabricated sensors [14,35,36]. Therefore, modifying directly-grown ZnO nanostructures with NiO QDs will improve not only the detection performance of nonenzymatic glucose sensor but also improve the stability of electrode.

In this work, we have fabricated, for the first time, the nonenzymatic flexible FET (f-FET) glucose sensor using ZnO NRs modified with NiO QDs on polyimide. The fabricated f-FET glucose sensor showed a wide-linear range and high sensitivity with good stability and repeatability during glucose detection. Rivaling the state-of-the-art nanomaterial based sensors; our designed nonenzymatic f-FET glucose sensor presents exciting potential for practical applications in clinical and industrial sectors.

2. Experimental details

2.1. Reagents

Zinc nitrate hexahydrate ($Zn(NO_3)_2{\cdot}6H_2O$, 99%), glucose (D-(+)-99.5%), hexamethylenetetramine (HMTA, 99%), cholesterol, uric acid (UA), ascorbic acid (AA), dopamine (DA), human blood serum (H4522), and 1.0 M phosphate buffered saline (PBS, pH 7.4) were purchased from Sigma-Aldrich and used as-obtained without further purification. Ultrapure de-ionized (DI) water (purified with Milli-Q plus system, Millipore Co.) with resistivity of ~18 MΩ cm and freshly prepared solutions were exclusively used in all aqueous solutions and measurements, respectively.

2.2. ZnO NRs synthesis, surface modification with NiO QDs and Characterization

To synthesized ZnO NRs, 0.01 M of $Zn(NO_3)_2{\cdot}6H_2O$ and 0.01 M HMTA were first dissolved in 50 mL of DI water and then transferred into a Pyrex glass bottle. The Pyrex glass bottle was heated in a laboratory oven for 4 h at 85 °C after suspending the seeded substrates upside down. After completion of the reaction, ZnO NRs grown electrodes were rinsed with DI water to remove any impurity and dried in air for further processing. The synthesized ZnO NRs were modified with NiO QDs using radio frequency (RF) magnetron sputtering. To modify ZnO NRs with NiO QDs, NiO target with 99.99 % purity was sputtered onto the pre-defined area at 60 W RF power in argon (Ar) atmosphere. The operation pressure in the sputter chamber was 7.2 $\times 10^{-5}$ torr, while the sputtering time was varied 10–50 s.

The morphology of as-synthesized ZnO NRs and NiO QDs modified ZnO NRs were characterized by field-emission scanning electron microscopy (FESEM, Carl Zeiss SUPRA 40 VP) equipped with energy dispersive spectroscopy (EDS) and transmission electron microscopy (TEM, JEOL-JEM-2010 equipped with CCD camera; operating voltage: 200 kV). The X-ray diffraction (XRD, Rigaku) patterns were measured with Cu-kα Radiation (λ = 1.54178 Å) at 40 kV.

2.3. Fabrication of nonenzymatic f-FET glucose sensor and electrical measurements

The fabrication process of the nonenzymatic f-FET glucose sensor is illustrated in Fig. 1. First, polyimide substrates were cleaned (i), followed by sputter deposition of Ag source-drain electrodes using Ag target (ii). Next, a thin ZnO seed layer was sputtered between source-drain using ZnO as a target (iii). Then, ZnO NRs were grown on the seeded layer (iv) by a low-temperature aqueous route (see Section 2.2 for details). Finally, the electrodes were insulated using PDMS leaving only active area, which reduces the leak current and prevents metal-nanorods contact (v). The NiO QDs were deposited on the grown ZnO NRs by RF sputter (vi).

The fabricated devices were measured using a data acquisition system (HP 4155A semiconductor parameter analyzer) for real-time data measurement. The direct current measurements were performed with two-terminal FET having a floating gate. The drain current (I_d) was recorded when the device was exposed to the different concentrations of glucose in the assigned gate voltage (V_g) range with a fixed drain-source voltage (V_{ds} = 0.0 V). The sensing tests were performed at room temperature using optimized 40 s deposited NiO QDs on ZnO NRs based nonenzymatic f-FET glucose sensor.

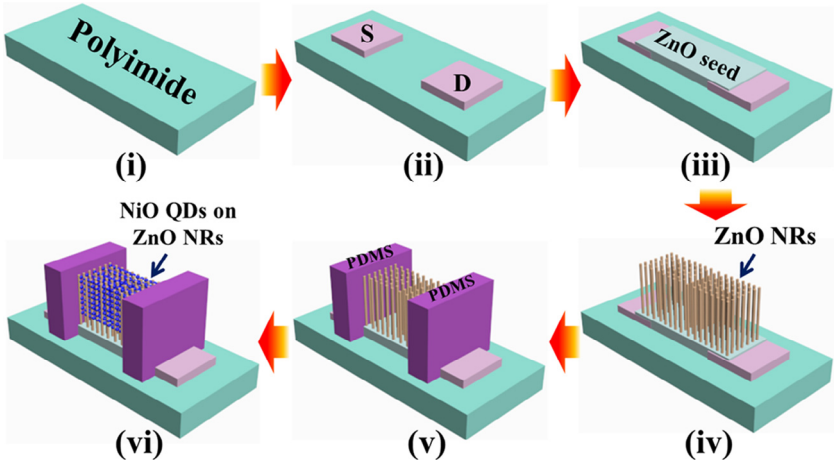

Fig. 1. Schematic illustrating the fabrication process of nonenzymatic f-FET glucose sensor. (i) Cleaned polyimide substrate; (ii) RF sputter deposited Ag source-drain electrodes; (iii) ZnO seed layer deposition using RF sputter; (iv) solution process growth of ZnO NRs; (v) PDMS covering; (vi) deposition of NiO QDs on ZnO NRs by RF sputter.

3. Results and discussion

3.1. Characterization of ZnO NRs and NiO QDs-modified ZnO NRs

Fig. 2a and b show the FESEM images of as-synthesized ZnO NRs surface and cross-sectional view. From the images, it can be seen that ZnO NRs are well-aligned perpendicularly to the substrate and grown in high density. Diameter and length of each nanorod are 70 ± 10 nm and 1.2 ± 0.15 μm, respectively. Fig. 2c and d present the low and high magnification TEM images of as-synthesized ZnO NR, respectively. The as-synthesized ZnO NR shows uniform and smooth surface. Fig. 2e and f exhibit the low and high magnification TEM images of the NiO QDs-modified ZnO NRs, respectively. Compared to the bare ZnO NRs, the NiO QDs-modified ZnO NRs have rough surface; the high resolution TEM image clearly shows that NiO QDs (~5 nm) are coated on the surface of ZnO NR (Fig. 2f). The high magnification TEM image shows the clear lattice fringes with the SAED patterns in the insets of Figs. 2c and 1e along with statistical line profile analysis (insets of Figs. 2d and 1f), respectively. It is seen that as-grown ZnO NR has lattice fringe of 0.26 nm, but the NiO QDs-coated ZnO NR shows reduced lattice fringe of 0.21 nm because of surface modification. The lattice fringes of ZnO NR correspond to the d-spacing of [0001] crystal plans, which is consistent with the bulk wurtzite crystal of ZnO and confirming that as-grown products are single crystalline and grown along the c-axis direction. The elemental mapping and EDS analysis (Fig. 3) confirm that the ZnO NRs are modified with NiO QDs. The EDX spectrum (Fig. 3e) demonstrates that the NiO QDs modified ZnO NRs contain Ni and Zn in the atomic ratio of Ni to Zn is about 1:15. The crystallinity of the as-grown ZnO NRs and after NiO QDs modification was examined by XRD (Fig. 4). All the diffraction peaks indicate that the ZnO NRs were highly oriented along c-axis perpendicular to the substrate surface showing no characteristic peak of any other impurities. Interestingly, XRD pattern of the NiO QDs modified ZnO NRs shows no additional peaks and/or peak shift, indicating that Ni^{2+} may be entered into the lattice of ZnO crystal due to the similar radius of the Ni^{2+} (0.72 Å) and Zn^{2+} (0.74 Å) [37].

3.2. Nonenzymatic glucose sensing using flexible FET sensor

3.2.1. Electrical characterizations

Fig. 5a presents the schematic of the fabricated f-FET based nonenzymatic glucose sensor consisting of NiO QDs modified ZnO NRs. Using this device configuration (device image is shown in inset of Fig. 5b); we measured the I_d-V_g characteristic of the optimized 40 s NiO QDs modified ZnO NRs in the absence/presence of 0.10 mM glucose in PBS buffer (0.10 M; pH 7.4) at an assigned V_g range of 0.0–2.0 V. The current was substantially increased with the glucose compared to that without it. The increase in current is considered to be due to the electrocatalytic reaction of the glucose over NiO QDs modified ZnO NRs. The electrochemical reactions of the Ni(III)/(II) are as follows [38–40]:

$$NiO + OH- \Rightarrow NiOOH + e- \quad (1)$$

$$NiOOH + glucose \Rightarrow Ni(OH)_2 + gluconolactone \quad (2)$$

$$2Ni(OH)_2 + O_2 \Rightarrow 2NiOOH + H_2O_2 \quad (3)$$

$$H_2O_2 \Rightarrow 2H^+ + O_2 + 2e- \quad (4)$$

where, H_2O molecules (or OH^-) are adsorbed on the surface of NiO through hydrogen bonding and leads to conversion of surface to hydroxide phase $Ni(OH)_2$. When electrodes are scanned at a higher potential, there is more conversion of NiO to $Ni(OH)_2$, and NiOOH in success (1). However, after glucose is introduced there is a reaction between NiOOH and glucose and as a result $Ni(OH)_2$ and gluconolactone are produced (2). The produced $Ni(OH)_2$ is further oxidized to form NiOOH and hydrogen peroxide (H_2O_2) at electrode surface (3). Finally, the electro-oxidation current of H_2O_2 is detected while applying the suitable potential to the system (4).

Under optimal experimental conditions (deposition effect of NiO QDs), the sensing tests were performed at room temperature using optimized 40 s deposited NiO QDs on ZnO NRs based nonenzymatic f-FET glucose sensor. The electrochemical performance of as-fabricated f-FETs was examined by I_d-V_g measurements in 0.10 M PBS buffer (pH 7.4). The I_d-V_g responses were measured in different glucose concentrations (0.001–50 mM). As shown in Fig. 6a, the current increases substantially from lower to higher concentration of glucose at room temperature. The increase in current is due to ions concentration increase and good electron communication throughout reaction. At a higher potential (~1.2 V), there is a noticeable current change which is due to the higher conversion of NiO to $Ni(OH)_2$ that leads to NiOOH production. To calculate the sensing performances, the average of response current were calculated in the 1.2–2.0 V range of for each sample and their corresponding calibration curve, i.e. response current *vs.* glucose concentration (mM) was drawn in log scale (Fig. 6b). From the calibrated current-concentration profile, the sensor showed two linear ranges of 0.001–10 mM and 10–50 mM with high regression coefficient

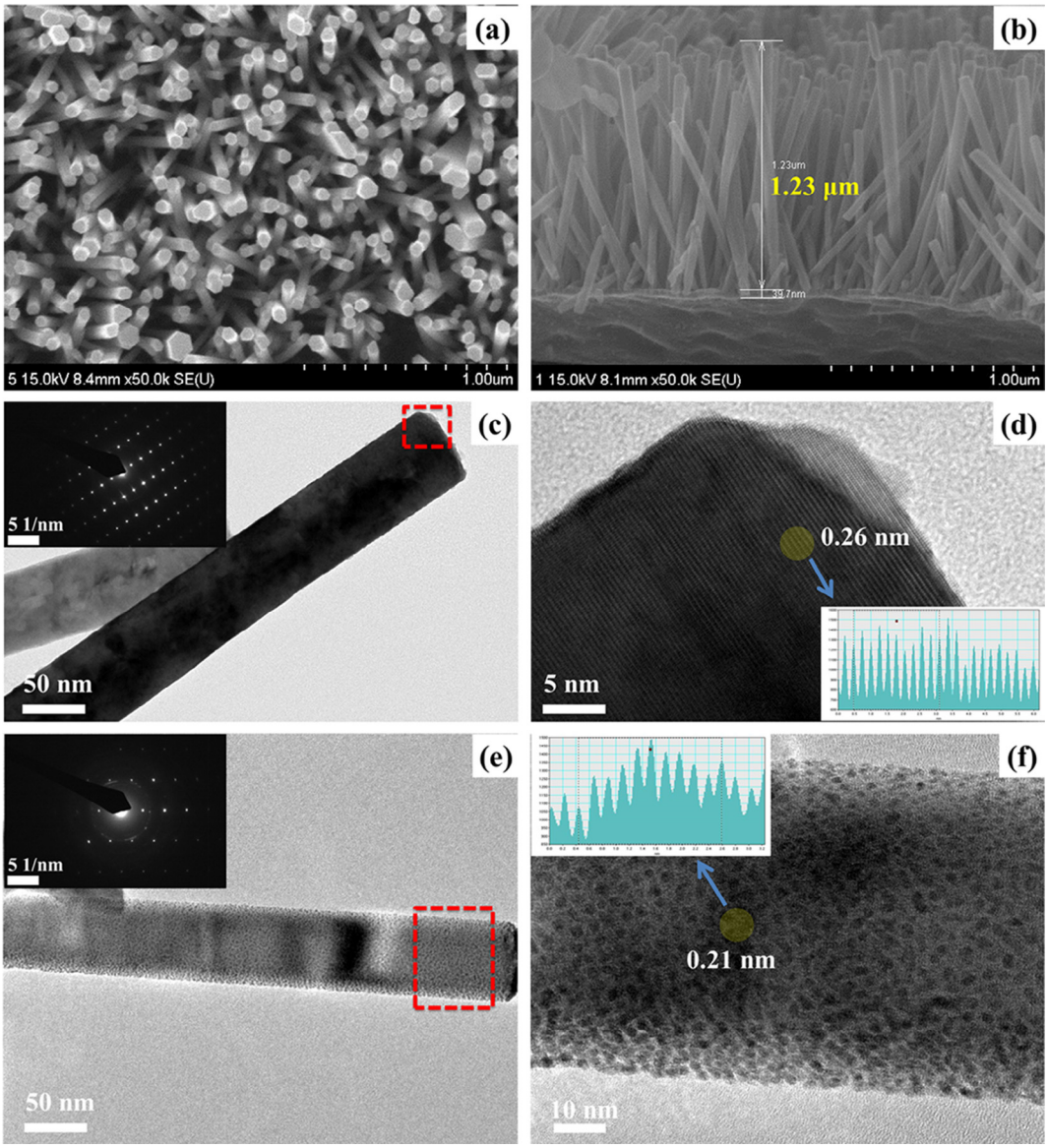

Fig. 2. Top- (a) and cross-sectional (b) FESEM images of as-synthesized ZnO NRs on polyimide substrate; low resolution TEM and HRTEM images of ZnO NR (c, d) and NiO QDs modified ZnO NR (e, f), respectively. Insets show the SAED patterns (c, e) and the lattice planes with statistical line profile analysis (d, f) of ZnO NR and NiO QDs modified ZnO NR.

(R^2) value of 0.9978 and 0.9997, respectively. The sensitivity of the sensor was calculated by the slope of each linear range. A higher sensitivity (13.14 μA cm^{-2} mM^{-1}) was obtained in the low concentration range (0.001–10 mM) of glucose, whereas at a higher concentration (10–50 mM) the sensitivity was 7.31 μA cm^{-2} mM mM^{-1}. A low limit of detection (LOD) was estimated to be 0.026 mM based on the standard deviation (SD) of the response and the slope (S) of the calibration curve, i.e. LOD = 3.3(SD/S). The sensing performance of the nonenzymatic sensor is compared with previously reported FET-based glucose sensors in Table 1.

3.2.2. Selectivity and stability test

To perform anti-interference test (Fig. 7), we prepared three samples in PBS solution i.e. sample (a) contains only 2.0 mM glucose, sample (b) contains 2.0 mM glucose and low concentration (0.1 mM) of each inferring species (AA, UA, cholesterol, and DA), and sample (c) contains 2.0 mM glucose and high concentration (0.5 mM) of each inferring species (AA, UA, cholesterol, and DA). The I_d-V_g responses of each sample are shown in Fig. 7 with calibrated histogram in inset. The current response of sensor in only glucose is almost similar to that of sample containing low concentration of interfering species ((physiological level). However, a slight decrease is noticed in the sample with high concentration of interfering species. This clearly shows that our fabricated sensors do not have any obvious effect on its performance in the presence of interfering species. Further, the stability and reproducibility of the fabricated sensors were accessed by repetitive measurements twice a week for 10 weeks. The sensor showed a high stability for glucose detection, which retained ~97 % of its original response after 8 weeks of storage. It suggests that our fabricated electrodes can be used favorably for the selective determination of glucose for several measurements.

3.3. Serum and blood samples analysis

For the direct application point of view, we analyzed response of our fabricated sensor in freshly drawn whole blood and filtered serum samples. The responses are shown in Fig. 8. The whole blood

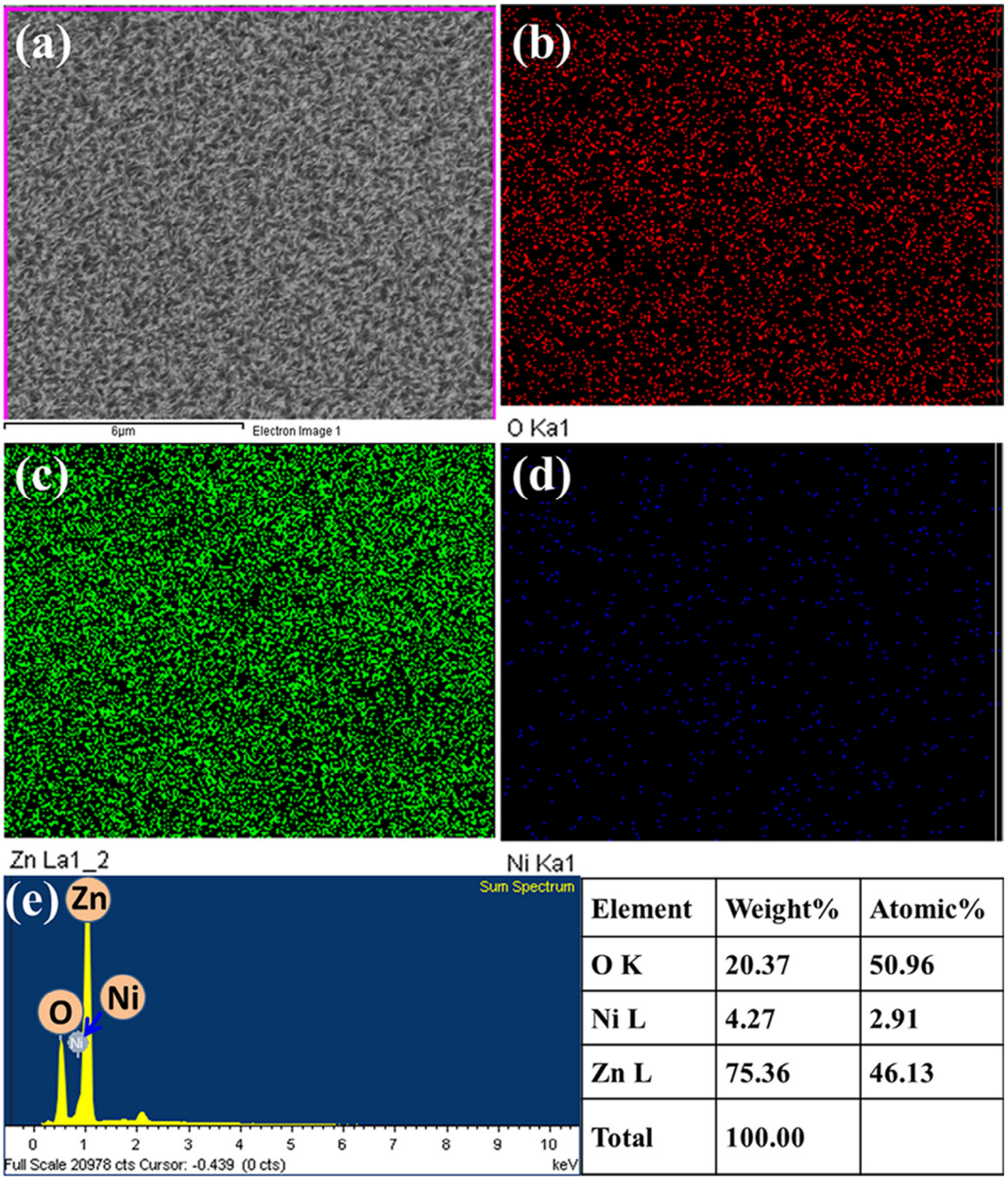

Element	Weight%	Atomic%
O K	20.37	50.96
Ni L	4.27	2.91
Zn L	75.36	46.13
Total	100.00	

Fig. 3. (a) FESEM image of NiO QDs decorated ZnO NRs; elemental mapping of (b) O, (c) Zn, and (d) Ni and (e) EDS spectra for FESEM image of ZnO NRs.

sample shows a slight decrease in the response, which may be due to presence of blood cells and protein fragments in the blood sample. However, we have noticed that the sensor recovers most of its response when it was removed from whole blood sample and tested in serum sample. Later, to check the accuracy and precision of our fabricated sensors, we measured the sensor response in known concentration of glucose in human serum samples (4.89 mM; Sigma-Aldrich, H4522). Furthermore, the reliability and repeatability of our fabricated sensors were checked by standard addition of pure glucose to the known concentration samples of human serum and the results are summarized in Table 2. Four samples were prepared after dilution in PBS buffer and each sample was analyzed three times to calculate their relative standard deviation (RSD) during measurements. In each sample 2.0 mM glucose was added and concentrations of standard additions were measured by our sensor. The relationship between added glucose concentration and the current response was generated and the

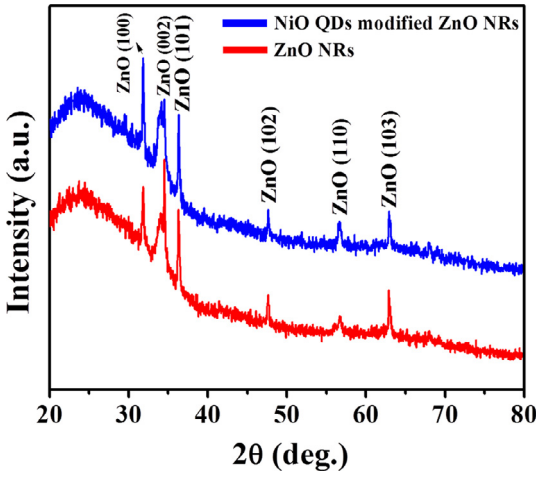

Fig. 4. XRD patterns of as-synthesized and NiO QDs modified ZnO NRs.

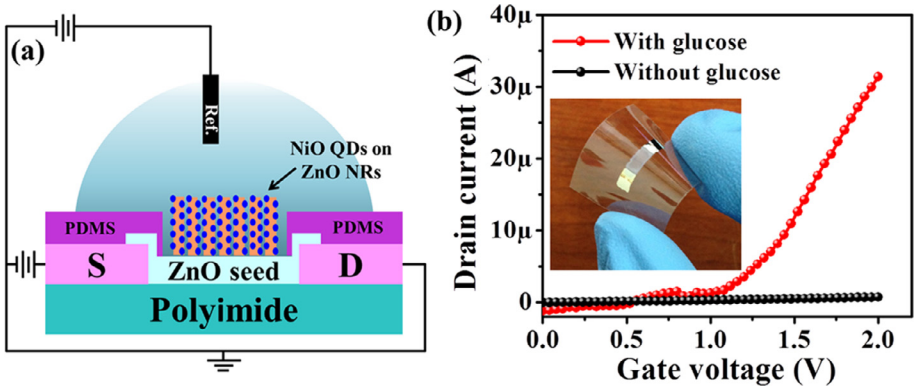

Fig. 5. (a) The schematic of nonenzymatic f-FET glucose sensor, (b) I_d-V_g response of nonenzymatic f-FET glucose sensor in the absence/presence of 0.10 mM glucose in 0.10 M PBS buffer (pH 7.4). Inset b shows an optical image of the nonenzymatic f-FET glucose sensor.

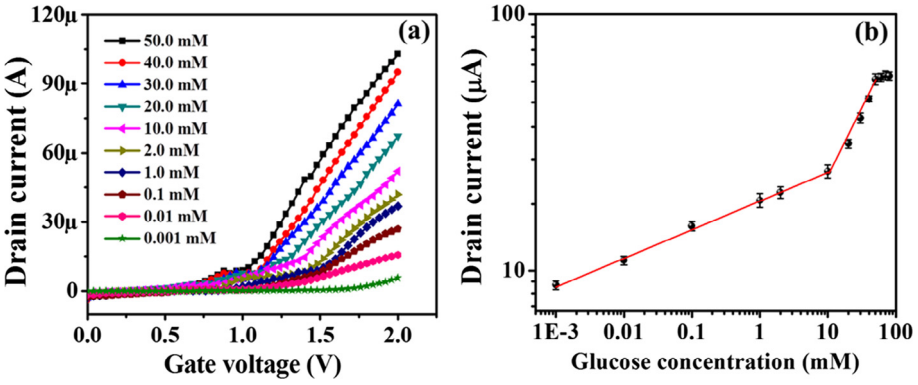

Fig. 6. (a) Typical I_d-V_g response with increasing glucose concentration (0.001–50 mM) and (b) their corresponding calibration curve, i.e. response current *vs.* glucose concentration (mM) in log scale. It showed two linear ranges of 0.001–10 mM and 10–50 mM with high regression coefficient (R^2) value of 0.9978 and 0.9997, respectively.

Table 1
Comparison of sensing performance with other reported FET-based glucose biosensors.

Electrode	Sensor type	Sensitivity (μA cm^{-2} mM^{-1})	Linear range (mM)	LOD (μM)	Ref.
Nf/GOx/ZnO NRs/Ag/PET	Enzymatic	22.3	0.0–80	70	[8]
Fe_2O_3-ZnO NRs/SiO_2/Si	Nonenzymatic	105.75	0.05–18	12	[14]
GOx-ZnO film/glass	Enzymatic	–	0.2–40	200	[41]
PANI-PAA/PANI-bisulfite/GOx-PDAB/Au	Enzymatic	0.001	–	–	[42]
GOx-ZnO NRs/SiO_2/Si	Enzymatic	32.27	0.05–70	0.07	[43]
GOx-silk-graphene/Silk film	Enzymatic	2.5	0.1–10	100	[44]
GOx-chitosan/Nf/PtNPs/graphene gate	Enzymatic	–	0.0005–1	0.5	[45]
GOx-PMMA/graphene/PET	Enzymatic	–	3.3–10.9	3.3	[46]
GOx/ZnO NWs/Au/PET	Enzymatic	19.5	0.2–2	50	[47]
GOx-CPNTs	Enzymatic	–	0.5–20	–	[48]
NiO QDs-ZnO NRs/Polyimide	Nonenzymatic	13.14	0.001–10	26	This work
NiO QDs-ZnO NRs/Polyimide	Nonenzymatic	7.31	10–50	26	This work

extrapolated curve used to determine glucose in the original sample. The percent recovery of the added glucose was also determined. The data obtained are in good agreement with the known concentration of glucose, showing that our fabricated sensor not only accurately measured glucose concentration in human serum samples but also exhibit good repeatability and reliability.

4. Conclusion

In this paper, for the first time, we fabricated the nonenzymatic f-FET based glucose sensor using ZnO NRs modified with NiO QDs between the source-drain on polyimide. The modification of ZnO NRs by NiO QDs not only increases the surface area but also enhance the electrocatalytic features. The fabricated f-FET nonenzymatic glucose sensor showed a wide-linear range, high sensitivity, and low detection limit. The fabricated sensor also showed high stability and reproducibility for glucose detection, indicating that our fabricated electrodes can be used favorably for the selective determination of glucose for several measurements. The human whole blood and serum samples analysis revealed that the nonenzymatic f-FET glucose sensor is capable of measuring glucose concentration in the presence of interfering species. Furthermore, accuracy and precision test in the serum sample presents exciting potential for practical applications in clinical and industrial sectors. Additionally, this simple and cheap, controllable method can be used for the mass production of affordable high performance nonenzymatic f-FET glucose sensors.

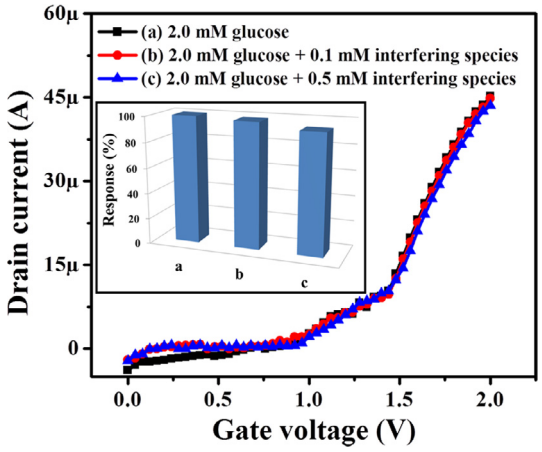

Fig. 7. Interference test. I_d-V_g response of nonenzymatic f-FET glucose sensor in (a) 2.0 mM glucose only, (b) 2.0 mM glucose containing 0.1 mM of each interfering species (AA, UA, cholesterol and DA), and (c) 2.0 mM glucose containing 0.5 mM of each interfering species (AA, UA, cholesterol and DA) in 0.10 M PBS buffer. Inset shows calibrated responses as histogram.

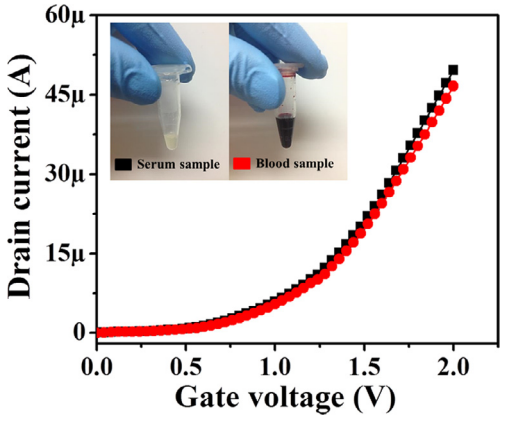

Fig. 8. Real sample analysis. I_d-V_g responses of nonenzymatic f-FET glucose sensor in human serum and whole blood samples. Inset shows the optical images of human blood and serum samples, respectively.

Table 2
Human serum sample analysis.

S. N.	Glucose conc. in serum (mM)	RSD (%) (n = 3)	Added glucose conc. (mM)	Measured glucose conc. (mM)	Recovery (%)
1	1.22	2.3	2.0	3.14	96
2	2.45	1.2	2.0	4.43	99
3	3.67	1.9	2.0	5.61	97
4	4.89	3.8	2.0	6.85	98

Acknowledgements

This work was supported by the National Leading Research Laboratory program through the National Research Foundation (NRF) (NRF-2016R1A2B2016665) of Korea funded by the Ministry of Science, ICT & Future Planning. Authors also thank KBSI, Jeonju branch for SEM analysis and Mr. Jong-Gyun Kang, Center for University Research Facility (CURF) for taking good quality TEM images.

References

[1] A. King, R.E. Aubert, W.H. Herman, Global burden of diabetes prevalence, numerical estimates and projections, Diabetes Care 21 (1998) 1414–1431.
[2] C.R. Gordijo, K. Koulajian, A.J. Shuhendler, L.D. Bonifacio, H.Y. Huang, S. Chiang, G.A. Ozin, A. Giacca, X.Y. Wu, Nanotechnology-enabled closed loop insulin delivery device: in vitro and in vivo evaluation of glucose-regulated insulin release for diabetes control, Adv. Funct. Mater. 21 (2011) 73–82.
[3] J.-S. Jang, S.-J. Choi, S.-J. Kim, M. Hakim, Kim. Il-Doo, Rational design of highly porous SnO_2 nanotubes functionalized with biomimetic nanocatalysts for direct observation of simulated diabetes, Adv. Funct. Mater. 26 (2016) 4740–4748.
[4] M.A. Pellitero, A. Guimerà, M. Kitsara, R. Villa, C. Rubio, B. Lakard, M.-L. Doche, J.-Y. Hihn, F.J. del Campo, Quantitative self-powered electrochromic biosensors, Chem. Sci. 8 (2017) 1995–2002.
[5] Y.-B. Hahn, R. Ahmad, N. Tripathy, Chemical and biological sensors based on metal oxide nanostructures, Chem. Commun. 48 (2012) 10369–10385.
[6] L.F. Ang, L.Y. Por, M.F. Yam, Development of an amperometric-based glucose biosensor to measure the glucose content of fruit, PLoS ONE 10 (2015) e0111859.
[7] B.K. Shrestha, R. Ahmad, H.M. Mousa, I.-G. Kim, J.I. Kim, M.P. Neupane, C. Hee Park, C.S. Kim, High-performance glucose biosensor based on chitosan-glucose oxidase immobilized polypyrrole/Nafion/functionalized multi-walled carbon nanotubes bio-nanohybrid film, J. Colloid Interface Sci. 482 (2016) 39–47.
[8] K.S. Bhat, R. Ahmad, J.-Y. Yoo, Y.-B. Hahn, Nozzle-jet printed flexible field-effect transistor biosensor for high performance glucose detection, J. Colloid Interface Sci. 506 (2017) 188–196.
[9] J. Song, L. Xu, C. Zhou, R. Xing, Q. Dai, D. Liu, H. Song, Synthesis of graphene oxide based CuO nanoparticles composite electrode for highly enhanced nonenzymatic glucose detection, ACS Appl. Mater. Interfaces 5 (2013) 12928–12934.
[10] R. Ahmad, N. Tripathy, Y.-B. Hahn, A. Umar, A.A. Ibrahimc, S.H. Kim, A robust enzymeless glucose sensor based on CuO nanoseed modified electrodes, Dalton Trans. 44 (2015) 12488–12492.
[11] Z. Ji, Y. Wang, Q. Yu, X. Shen, N. Li, H. Ma, J. Yang, J. Wang, One-step thermal synthesis of nickel nanoparticles modified graphene sheets for enzymeless glucose detection, J. Colloid Interface Sci. 506 (2017) 678–684.
[12] W. Wang, L. Kong, J. Zhu, L. Tan, One-pot preparation of conductive composite containing boronic acid derivative for non-enzymatic glucose detection, J. Colloid Interface Sci. 498 (2017) 1–8.
[13] Q. Wang, X. Zhang, L. Huang, Z. Zhang, S. Dong, One-pot synthesis of Fe3O4 nanoparticle loaded 3D porous graphene nanocomposites with enhanced nanozyme activity for glucose detection, ACS Appl. Mater. Interfaces 9 (2017) 7465–7471.
[14] R. Ahmad, M.-S. Ahn, Y.-B. Hahn, Fabrication of a non-enzymatic glucose sensor field-effect transistor based on vertically-oriented ZnO nanorods modified with Fe_2O_3, Electrochem. Commun. 77 (2017) 107–111.
[15] L.Y. Chen, T. Fujita, Y. Ding, M.W. Chen, A three-dimensional gold-decorated nanoporous copper core-shell composite for electrocatalysis and nonenzymatic biosensing, Adv. Funct. Mater. 20 (2010) 2279–2285.
[16] S. Wang, J. Sun, Y. Jia, L. Yang, N. Wang, Y. Xianyu, W. Chen, X. Li, R. Cha, X. Jiang, Nanocrystalline cellulose-assisted generation of silver nanoparticles for nonenzymatic glucose detection and antibacterial agent, Biomacromolecules 17 (2016) 2472–2478.
[17] R. Ahmad, M. Vaseem, N. Tripathy, Y.-B. Hahn, Wide linear-range detecting nonenzymatic glucose biosensor based on CuO nanoparticles inkjet-printed on electrodes, Anal. Chem. 85 (2013) 10448–10454.
[18] M. Sivakumar, R. Madhu, S.-M. Chen, V. Veeramani, A. Manikandan, W.H. Hung, N. Miyamoto, Y.-L. Chueh, Low-temperature chemical synthesis of $CoWO_4$ nanospheres for sensitive nonenzymatic glucose sensor, J. Phys. Chem. C 120 (2016) 17024–17028.
[19] S. Fu, C. Zhu, J. Song, M. Engelhard, H. Xia, D. Du, Y. Lin, PdCuPt nanocrystals with multibranches for enzyme-free glucose detection, ACS Appl. Mater. Interfaces 8 (2016) 22196–22200.
[20] Z. Amani-Beni, A. Nezamzadeh-Ejhieh, A novel non-enzymatic glucose sensor based on the modification of carbon paste electrode with CuO nanoflower: designing the experiments by response surface methodology (RSM), J. Colloid Interface Sci. 504 (2017) 186–196.
[21] N.Q. Dung, D. Patil, H. Jung, D.A. Kim, A high-performance nonenzymatic glucose sensor made of CuO-SWCNT nanocomposites, Biosens. Bioelectron. 42 (2013) 280–286.
[22] J. Wang, L. Xu, Y. Lu, K. Sheng, W. Liu, C. Chen, Y. Li, B. Dong, H. Song, Engineered IrO_2@NiO core-shell nanowires for sensitive non-enzymatic detection of trace glucose in saliva, Anal. Chem. 88 (2016) 12346–12353.
[23] X. Niu, M. Lan, H. Zhao, C. Chen, Highly sensitive and selective nonenzymatic detection of glucose using three-dimensional porous nickel nanostructures, Anal. Chem. 85 (2013) 3561–3569.
[24] W. Lu, X. Qin, A.M. Asiri, A.O. Al-Youbi, X. Sun, Ni foam: a novel three-dimensional porous sensing platform for sensitive and selective nonenzymatic glucose detection, Analyst 138 (2013) 417–420.
[25] S. Ci, T. Huang, Z. Wen, S. Cui, S. Mao, D.A. Steeber, J. Chen, Nickel oxide hollow microsphere for non-enzyme glucose detection, Biosens. Bioelectron. 54 (2014) 251–257.
[26] P. Yang, X. Tong, G. Wang, Z. Gao, X. Guo, Y. Qin, NiO/SiC nanocomposite prepared by atomic layer deposition used as a novel electrocatalyst for

nonenzymatic glucose sensing, ACS Appl. Mater. Interfaces 7 (2015) 4772–4777.
[27] C. Chen, D. Liu, W. Lu, K. Wang, G. Du, A.M. Asiri, X. Sun, Three-dimensional Ni_2P nanoarray: an efficient catalyst electrode for sensitive and selective nonenzymatic glucose sensing with high specificity, Anal. Chem. 88 (2016) 7885–7889.
[28] N. Karikalan, M. Velmurugan, S.-M. Chen, C. Karuppiah, Modern approach to the synthesis of $Ni(OH)_2$ decorated sulfur doped carbon nanoparticles for the nonenzymatic glucose sensor, ACS Appl. Mater. Interfaces 8 (2016) 22545–22553.
[29] H. Gao, F. Xiao, C.B. Ching, H. Duan, One-step electrochemical synthesis of PtNi nanoparticle-graphene nanocomposites for nonenzymatic amperometric glucose detection, ACS Appl. Mater. Interfaces 3 (2011) 3049–3057.
[30] K.-C. Lin, Y.-C. Lin, S.-M. Chen, A highly sensitive nonenzymatic glucose sensor based on multi-walled carbon nanotubes decorated with nickel and copper nanoparticles, Electrochimica Acta 96 (2013) 164–172.
[31] M. Wu, S. Meng, Q. Wang, W. Si, W. Huang, X. Dong, Nickel-cobalt oxide decorated three-dimensional graphene as an enzyme mimic for glucose and calcium detection, ACS Appl. Mater. Interfaces 7 (2015) 21089–21094.
[32] W. Dai, H. Li, M. Li, C. Li, X. Wu, B. Yang, Electrochemical imprinted polycrystalline nickel-nickel oxide half-nanotube-modified boron-doped diamond electrode for the detection of L-serine, ACS Appl. Mater. Interfaces 7 (2015) 22858–22867.
[33] Y.-B. Hahn, Zinc oxide nanostructures and their applications, Korean J. Chem. Eng. 28 (2011) 1797–1813.
[34] Y. Qiao, J. Li, H. Li, H. Fang, D. Fan, W. Wang, A label-free photoelectrochemical aptasensor for bisphenol A based on surface plasmon resonance of gold nanoparticle-sensitized ZnO nanopencils, Biosens. Bioelectron. 86 (2016) 315–320.
[35] R. Ahmad, N. Tripathy, M.-S. Ahn, Y.-B. Hahn, Solution process synthesis of high aspect ratio ZnO nanorods on electrode surface for sensitive electrochemical detection of uric acid, Sci. Rep. 7 (2017) 46475.
[36] R. Ahmad, N. Tripathy, M.Y. Khan, K.S. Bhat, M.-S. Ahn, Y.-B. Hahn, Ammonium ion detection in solution using vertically grown ZnO nanorod based field-effect transistor, RSC Adv. 6 (2016) 54836–54840.
[37] X. Chu, X. Zhu, Y. Dong, T. Chen, M. Ye, W. Sun, An amperometric glucose biosensor based on the immobilization of glucose oxidase on the platinum electrode modified with NiO doped ZnO nanorods, J. Electroanal. Chem. 676 (2012) 20–26.
[38] Y. Mu, D. Jia, Y. He, Y. Miaoa, H.-L. Wu, Nano nickel oxide modified non-enzymatic glucose sensors with enhanced sensitivity through an electrochemical process strategy at high potential, Biosens. Bioelectron. 26 (2011) 2948–2952.
[39] Y. Ding, Y. Liu, J. Parisi, L. Zhang, Y. Lei, A novel NiO-Au hybrid nanobelts based sensor for sensitive and selective glucose detection, Biosens. Bioelectron. 28 (2011) 393–398.
[40] N.Q. Dung, D. Patil, H. Jung, J. Kim, D. Kim, NiO-decorated single-walled carbon nanotubes for high-performance nonenzymatic glucose sensing, Sens. Actuators B 183 (2013) 381–387.
[41] K. Koike, Y. Mori, S. Sasa, Y. Hirofuji, M. Yano, Glucose sensing by an enzyme-modified ZnO-based FET, Proc. Eng. 168 (2016) 84–88.
[42] E.S. Forzani, H. Zhang, L.A. Nagahara, I. Amlani, R. Tsui, N. Tao, A conducting polymer nanojunction sensor for glucose detection, Nano Lett. 4 (2004) 1785–1788.
[43] R. Ahmad, N. Tripathy, J.-H. Park, Y.-B. Hahn, A comprehensive biosensor integrated with a ZnO nanorod FET array for selective detection of glucose, cholesterol and urea, Chem. Commun. 51 (2015) 11968–11971.
[44] X.Y. James, J. Pak, Graphene-based field effect transistor enzymatic glucose biosensor using silk protein for enzyme immobilization and device substrate, Sens. Actuators B: Chem. 202 (2014) 1357–1365.
[45] M. Zhang, C. Liao, C.H. Mak, P. You, C.L. Mak, F. Yan, Highly sensitive glucose sensors based on enzyme-modified whole-graphene solution-gated transistors, Sci. Rep. 5 (2015) 8311.
[46] Y.H. Kwak, D.S. Choi, Y.N. Kim, H. Kim, D.H. Yoon, S.-S. Ahn, J.-W. Yang, W.S. Yang, S. Seo, Flexible glucose sensor using CVD-grown graphene-based field effect transistor, Biosens. Bioelectron. 37 (2012) 82–87.
[47] D. Pradhan, F. Niroui, K.T. Leung, High-performance, flexible enzymatic glucose biosensor based on ZnO nanowires supported on a gold-coated polyester substrate, ACS Appl. Mater. Interfaces 2 (2010) 2409–2412.
[48] H. Yoon, S. Ko, J. Jang, Field-effect-transistor sensor based on enzyme-functionalized polypyrrole nanotubes for glucose detection, J. Phys. Chem. B 112 (2008) 9992–9997.